INSTITUTE OF PHYSICS PUBLISHING JOURNAL OF OPTICS A: PURE AND APPLIED OPTICS

J. Opt. A: Pure Appl. Opt. **4** (2002) S356–S363 PII: S1464-4258(02)36815-6

A twofold modulation frequency laser range finder

Stéphane Poujouly and Bernard Journet

SATIE (CNRS UMR-8029)/ENS Cachan, 61 Ave Pdt Wilson, 94230 Cachan, France

E-mail: bernard.journet@satie.ens-cachan.fr

Received 8 May 2002
Published 4 November 2002
Online at stacks.iop.org/JOptA/4/S356

Abstract
The purpose of this paper is to present the conception of a twofold modulation frequency laser range finder. The system is based on the phase-shift measurement method with two modulation frequencies, one giving the distance within a wide range and a second one leading to high resolution measurement. The measurement method is based on intermediate frequency sampling associating the under-sampling technique with digital synchronous detection. Its main advantage is a global simplification of the electronic system, leading to a quite simple development and low cost system. There is only one phase-shift measurement stage but the twofold modulation frequency is possible thanks to the heterodyne technique. The emission and detection parts are designed for wideband operation and are digitally controlled. The whole system has been designed with only one digital phase locked loop reducing the phase noise and improving the resolution. Because of the global structure and the different digitally controlled parts the necessary calibration process could be introduced. From the design of the prototype it is possible to move towards a smart laser range finder.

Keywords: Laser range finding, phase-shift measurement, under-sampling technique, digital synchronous detection, smart sensor, electronic imaging

(Some figures in this article are in colour only in the electronic version)

1. Introduction

Laser range-finder based systems are now powerful and various methods have been developed [1]. They are dedicated to indoor robotics [2], non-destructive testing, inspection and security control or automotive intelligent cruise control [3]. Beside triangulation or interferometric methods there is a large place for flight time measurement methods implemented with pulse or phase-shift measurement. By the use of the heterodyne technique [4], phase-shift measurement leads to the conversion of a short time interval, at the modulation frequency, to a larger time interval more suitable for measurement. For a given phase-shift measurement resolution the distance resolution depends on the modulation frequency, but this frequency leads also to a non-ambiguity range because of the 2π modulo in phase estimation. The expressions for the time of flight, the corresponding phase-shift, the non-ambiguity range and the resolution are recalled below:

$$\tau_d = \frac{2d}{c} \tag{1}$$

$$\psi_d = 2\pi f_0 \tau_d \tag{2}$$

$$d_{nar} = \frac{c}{2f_0} \tag{3}$$

$$\delta d = \frac{c}{4\pi f_0}\delta\psi. \tag{4}$$

Equations (3) and (4) show that if a high modulation frequency is necessary to improve the resolution, it will also decrease the non-ambiguity range. A solution to solve this trade-off is to introduce a twofold modulation frequency, the lower frequency giving the distance within a wide range, and the higher leading to high resolution for the final distance estimation.

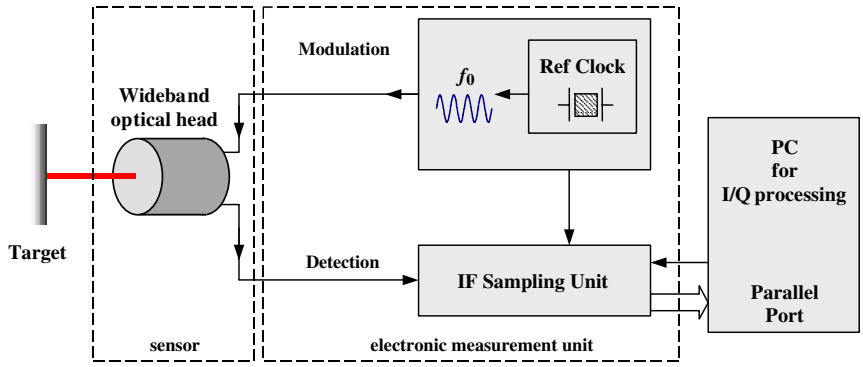

Figure 1. Block diagram of the laser range finder.

The organization of the prototype is presented in figure 1. The optical power of a laser diode output beam is continuously modulated by means of the forward current modulation. After reflection on the target the optical signal is focused on the detector. Both emitted and detected signals have to be compared leading to phase-shift estimation. The emission and detection parts, associated with the optical components, form the optical head. The electronic measurement unit produces the modulating signal and performs the digital acquisition of the signals to be compared, the comparison being achieved according to the measurement technique. Then phase-shift estimation is realized by a PC linked to the electronic measurement unit through the parallel port. Such a system could be applied to environment monitoring, non-destructive testing or indoor robotics.

2. The optical head

As shown in figure 2, the optical head is designed with only one optical axis, by using a small periscope.

2.1. The emission part

The emission part associates the laser diode, a bias section with a control loop to stabilize the output power versus the temperature, and the modulation section. The bias point, fixing the average output power, is digitally tuned from the PC through a serial bus. The system may be suited to different kinds of laser diode, depending on the average output power, on the threshold current and on the monitoring photodiode current. For convenience we have chosen to work with red light, and different laser diodes have been used, from Toshiba, Sony or SDL, with output power from 3 to 30 mW.

Because of the different modulation frequencies a wide-band structure is required. An integrated circuit, the OPA2662 from TI/Burr Brown containing two transconductance amplifiers with a 370 MHz bandwidth and up to 75 mA output current, drives the laser diode for both biasing point and modulating current injection. The amplitude of the modulation signal is digitally controlled by means of a digital trim gain amplifier, the CLC5506 from National Semiconductor, with 600 MHz bandwidth and a tuning range from 10 to 26 dB. Thus it is possible to adjust the modulating signal, according to the bias current, for the best dynamic with a linear behaviour, and for improving the signal to noise ratio.

2.2. Optical components

An important problem concerns the focusing of the output beam. As the output beam of a laser diode is highly divergent, at least one focusing lens is absolutely necessary, that is the present configuration for the prototype. But with a standard lens the focusing is not very efficient for a wide range such as 15 m. It would be better to use a pigtailed semiconductor laser, or to link the laser diode beam into a glass fibre by an optical system [5]. In this way it could also be possible to move the emission board to a more convenient position on the prototype.

The focusing lens is an aspheric lens with 50 mm focal length and a wide 68 mm diameter to catch a maximum of light, improving the signal to noise ratio at the output of the detector. The position of this lens can be tuned by hand but a motorized tuning could be introduced. An interferential filter can also be used to avoid detector blooming.

2.3. The detection part

The detector is based on an avalanche photodiode (APD), the S2382 from Hamamatsu, and a low noise amplifier, another CLC5506. The gain of the amplifier is digitally controlled during the measurement process depending on the observed signal. The APD is biased with a very compact high voltage module, the HAPM 0.2PS from Matsusada, included in a control loop. There is no selective filter because of the expected twofold frequency modulation system.

3. The IF sampling method

For a given modulation frequency there are mainly two methods to determine the phase-shift between emitted and detected signals. The first possibility is based on the heterodyne process, leading to a larger time interval than in the case of direct measurement [4]. The second possibility is synchronous detection, leading to the detection of two continuous quantities, related to the phase-shift and to the amplitude of the detected signal. The intermediate frequency (IF) sampling method proposed here was first developed for radio-communications. It associates the under-sampling technique with digital synchronous detection [6].

The use of this technique is very interesting because of a system simplification, specially by moving the digitization process closer to the sensor which is the optical head.

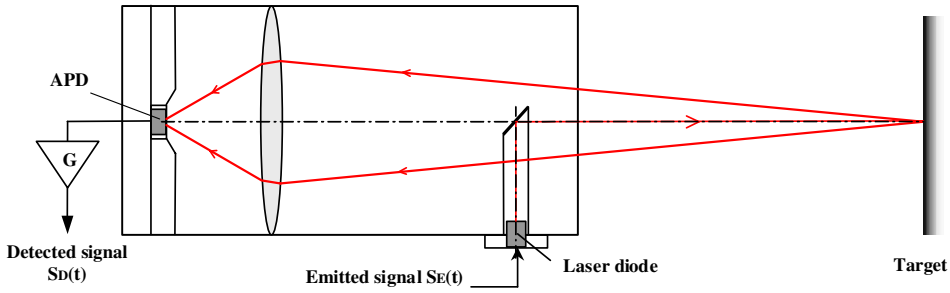

Figure 2. The optical head.

Otherwise under-sampling acts as the heterodyne technique moving the phase measurement process towards lower frequency values. Another interest of the under-sampling process is to avoid the use of high sampling frequency that is always difficult to perform and is rather expensive [7].

The signal modulating the optical power of the output beam is considered the emitted signal and is given by

$$s_E(t) = \hat{S}_E \cos(\omega_0 t). \tag{5}$$

The detected signal is obtained after propagation, reflection on the target, and demodulation by the APD.

$$s_D(t) = \hat{S}_D \cos(\omega_0 t + \psi_d + \phi_e). \tag{6}$$

In equation (6) ϕ_e is a global opto-electronic phase-shift due to emission and reception delay at the modulation frequency, and ψ_d is the phase-shift due to the optical flight and containing the distance information. The emitted signal is considered to be globally attenuated from emission to detection; this effect is taken into account by an attenuation coefficient α such as $\hat{S}_D = \alpha \hat{S}_E$. It is important to notice that α mainly depends on the target surface but also on the propagation path of the optical wave and on the opto-electronic emission and detection effects.

3.1. Under-sampling

The under-sampling process is presented in the frequency domain in figure 3. The initial signal at the modulation frequency f_0, after detection, is polluted by noise. Firstly it is narrowband filtered as shown in figure 3(a), in order to fit the Shannon theorem, specifying that the digitization of a signal requires a sampling frequency that is greater than twice the bandwidth of the signal. During the sampling process there is a periodization at each multiple of the sampling frequency which is denoted f_{SP} (figure 3(b)). If nf_{SP} is the closest frequency to f_0 then $f_0 - nf_{SP} = f_{AL}$ is the lowest spectral component. After mixing with a signal at this f_{AL} frequency a DC component is obtained and may be selected by low pass filtering as shown in figure 3(c).

The detected signal after digitization is denoted

$$s_D[k] = \alpha \hat{S}_E \cos[2\pi f_0 k T_{SP} + (\psi_d + \phi_e)]. \tag{7}$$

3.2. Digital synchronous detection

As for analog synchronous detection the signal to be analysed has to be mixed with two digital reference signals in quadrature [7], denoted RI for in phase and RQ for in quadrature.

$$RI[k] = \sin[2\pi f_{AL} k T_{SP}] \tag{8}$$

$$RQ[k] = \cos[2\pi f_{AL} k T_{SP}]. \tag{9}$$

The mixing of $s_D[k]$ with $RI[k]$ and $RQ[k]$ leads to the measured quantities $MI[k]$ and $MQ[k]$.

A very interesting simplification of the multiplication process may occur with an appropriate choice of the aliased frequency f_{AL}, that means in fact an appropriate choice of the sampling frequency. So if $2\pi f_{AL} k T_{SP} = k\pi/2$ then the values of $RI[k] = \sin(k\pi/2)$ and $RQ[k] = \cos(k\pi/2)$ are only 1, 0 or -1 and the multiplication may be performed by a simple programmable logic device. The corresponding condition for the sampling frequency is

$$f_{SP} = \frac{4 f_0}{4p + 1}. \tag{10}$$

Therefore $MI[k]$ and $MQ[k]$ are defined in the following table.

k odd	$MI[k] = \alpha \hat{S}_E \times \sin(\psi_d + \phi_e)$	$MQ[k] = 0$
k even	$MI[k] = 0$	$MQ[k] = \alpha \hat{S}_E \times \cos(\psi_d + \phi_e)$

From $MI[k]$ and $MQ[k]$ it is easy to obtain the global phase-shift $\psi_d + \phi_e$ and the attenuation coefficient α. The electronic phase-shift ϕ_e must be determined by calibration. From both α and ψ_d measurements on the whole target it is possible to reconstruct an image in terms of position but also of surface aspect, by grey level coding [9], leading to electronic imaging.

3.3. Feasibility of the method

A test board has been realized for validation of the IF sampling process and phase-shift measurement method. It has been designed for $f_0 = 10$ MHz and $f_{SP} = 8$ MHz (corresponding to the case $p = 1$ and $f_{AL} = 2$ MHz), and is presented in figure 4. The inboard clock reference is at 80 MHz. The band-pass filter is a sixth order LC filter. The analog to digital converter (ADC) is the ADS805 (12 bits/20 mega samples s^{-1}) from TI/Burr-Brown. The digital synchronous detection is achieved by a simple programmable logic device, an ispLSI1016 from Lattice-SC.

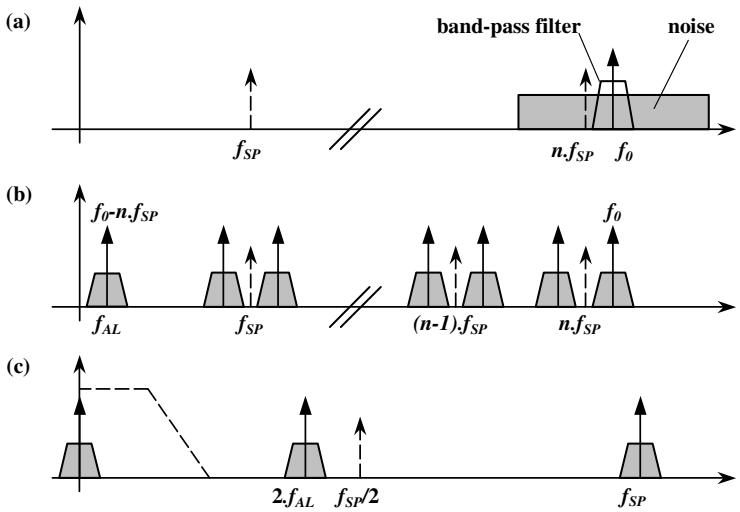

Figure 3. Representation of the signals in the frequency domain. (*a*) Signal at the output of the detector. (*b*) Signal after digitization at the sampling frequency. (c) Signal after mixing by a component at frequency f_{AL}.

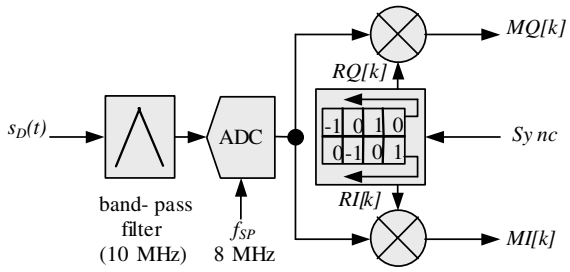

Figure 4. The board to be tested.

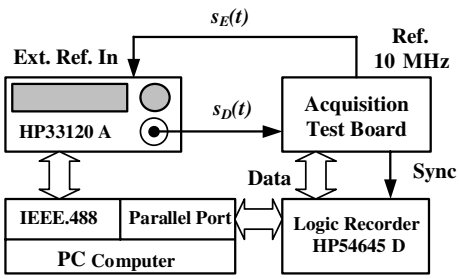

Figure 5. Set-up for IF sampling process testing.

The experimental set-up is presented in figure 5.

From the clock reference, the 10 MHz signal is used to produce $s_E(t)$, and to synchronize a highly stable synthesized waveform generator outputting the phase-shifted signal $s_D(t)$. After the mixing process, the data are collected by a logic recorder and transmitted to the PC for averaging and phase-shift estimation. The PC is also used by the way of an IEEE.488 interface board to tune the phase-shift on the waveform generator. So it is possible to compare the tuned phase-shift and the measured one.

The first results are presented in figure 6; the phase-shift measurement error is plotted as a function of the tuned phase-shift. The standard deviation is only 0.12° for a maximum value of 0.24°, proving the feasibility of the method.

The interest of the under-sampling technique may be underlined here. The standard deviation in phase-shift

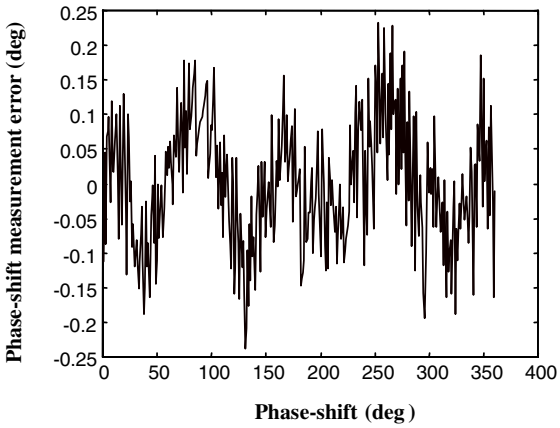

Figure 6. Phase-shift measurement results.

estimation depends on the quantum of the analog to digital conversion and on the sampling clock jitter. The phase error is $\delta\varphi_{err} \approx 2\pi f_0 \tau_j$, where τ_j is the time jitter of the clock which is approximately 5 ps. So at $f_0 = 10$ MHz, $\delta\varphi_{err} = 0.018°$, which is a good result (5×10^{-5} as relative error), but at $f_0 = 100$ MHz the phase error would be $\delta\varphi_{err} = 0.18°$ and at $f_0 = 240$ MHz it would be $\delta\varphi_{err} = 0.43°$. That would be the case for high frequency direct sampling. With the under-sampling technique the standard deviation is only 0.12°.

3.4. The IF sampling unit

The whole IF sampling unit is presented in figure 7.

A gain controlled input amplifier (once again a CLC5506) is placed at the input of the unit in order to keep a fairly constant amplitude for the signal and thus the best dynamic for filtering and digitization.

The low pass filtering could be obtained by a digital filtering technique such as decimation filters leading also to data rate reduction. Such filters require large programmable gate array circuits [10], but a simple averaging process, for example up to 8192 samples, is enough for filtering and for

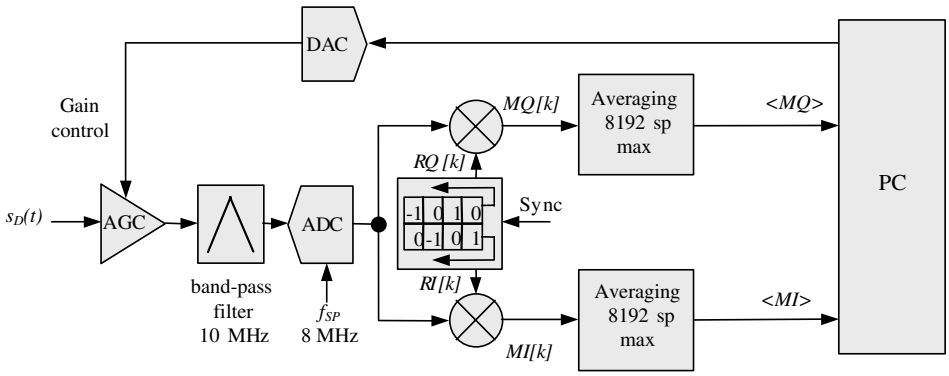

Figure 7. The whole IF sampling unit.

data rate reduction; otherwise it can be performed by a second simple programmable logic device. The averaged I and Q data are then transmitted to the PC through the parallel port (24-bit format, so eight bits at a time), for I/Q processing and distance determination. This averaging process and the digital interface to the parallel port of the PC have been realized and tested.

4. The twofold modulation frequency system

4.1. Principle of operation

The first modulation frequency has been chosen here at $f_{0L} = f_0 = 10$ MHz, leading to 15 m for the non-ambiguity range. Considering 0.2° resolution for phase measurement, the resolution is 1 cm at f_{0L}. Introducing a second high modulation frequency at $f_{0H} = 240$ MHz the non-ambiguity range is 63 cm but the resolution is improved by 24, becoming 0.35 mm.

As has been seen previously, the IF sampling unit is designed with the narrowband filter, for an input signal at 10 MHz and a sampling frequency of 8 MHz. It is an interesting way to reduce the cost of the system to have only one IF sampling unit. The solution is to move the high frequency towards 10 MHz by the heterodyne technique, this frequency acting as the IF of this process. So the local oscillator frequency is chosen at $f_{LO} = 230$ MHz. The organization of the twofold modulation system is shown in figure 8.

The twofold frequency measurement is performed sequentially, one switch being used to select the modulation signal and two switches being used to select which one of the corresponding 10 MHz return signals is placed at the input of the IF sampling unit.

It is necessary to synthesize the different frequencies with a minimum number of phase locked loops (PLLs), avoiding an increase of the phase noise, which is critical for phase-shift measurement at high accuracy. With a clock reference at $f_{CK} = 80$ MHz, the high modulation frequency $f_{0H} = 240$ MHz is obtained by filtering and amplifying the third harmonic of the square signal. The low modulation frequency $f_{0L} = 10$ MHz is obtained by dividing f_{CK} by eight and filtering with the same kind of filter as for the IF sampling unit; the sampling frequency $f_{SP} = 8$ MHz is obtained by dividing f_{CK} by ten.

The 230 MHz local oscillator frequency must be synthesized by a PLL but it is important to notice there is only one PLL in the global structure, which is a very important improvement compared with analog heterodyne systems [4]. This PLL is designed in order to reduce the phase noise of the oscillator and so the global noise. The choice is the digital PLL MA1017 from Philips, including both the programmable divider and the phase comparator in only one case, reducing the number of circuits, and with a charge pump technology for the phase comparator avoiding the use of active filters. The voltage controlled oscillator (VCO) is a MAX2620, which is a very low cost circuit from Maxim chosen because of its slope being less than 1 MHz V^{-1}. Thus 1 mV noise at the input of the VCO induces only a 1 kHz glitch.

4.2. Organization of the prototype

The whole structure of the prototype is presented in figure 8. The five blocks are plugged on a mother board with one bus for the power supply lines and one bus for the digital control of each block.

5. Measurement accuracy

The measurement accuracy depends on external conditions determining the level of the detected signal and on internal characteristics of the prototype, that are the intrinsic performances of the method and the behaviour of the system versus temperature drift.

5.1. Influence of the detected signal

The amplitude of the detected signal depends on the distance to be estimated and on the kind of target. It could be interesting to increase the output power of the system but this power is limited by safety regulation and operating conditions.

According to the European Norm EN-60-825, in the case of professional use a class 3A product is allowed, and for continuous operation the maximum average output power is 5 mW. If the operation is limited to 1 ms the output power can be 20 mW, but the power improvement is only 6 dB. For class 2 products the continuous operation is limited to 1 mW output power and for 1 ms operating time it could be 4 mW. The structure of the prototype presented in this paper enables such a process, and in 1 ms it is possible to make a complete

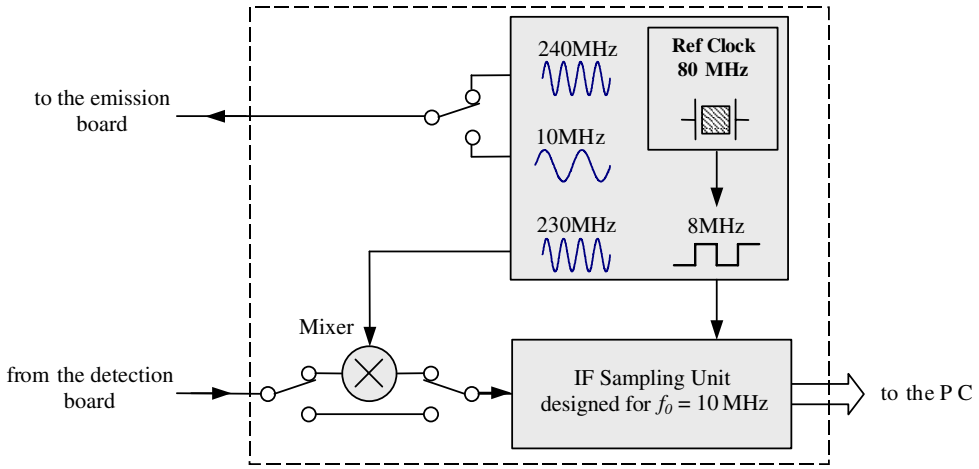

Figure 8. Principle of the twofold modulation frequency laser range finder.

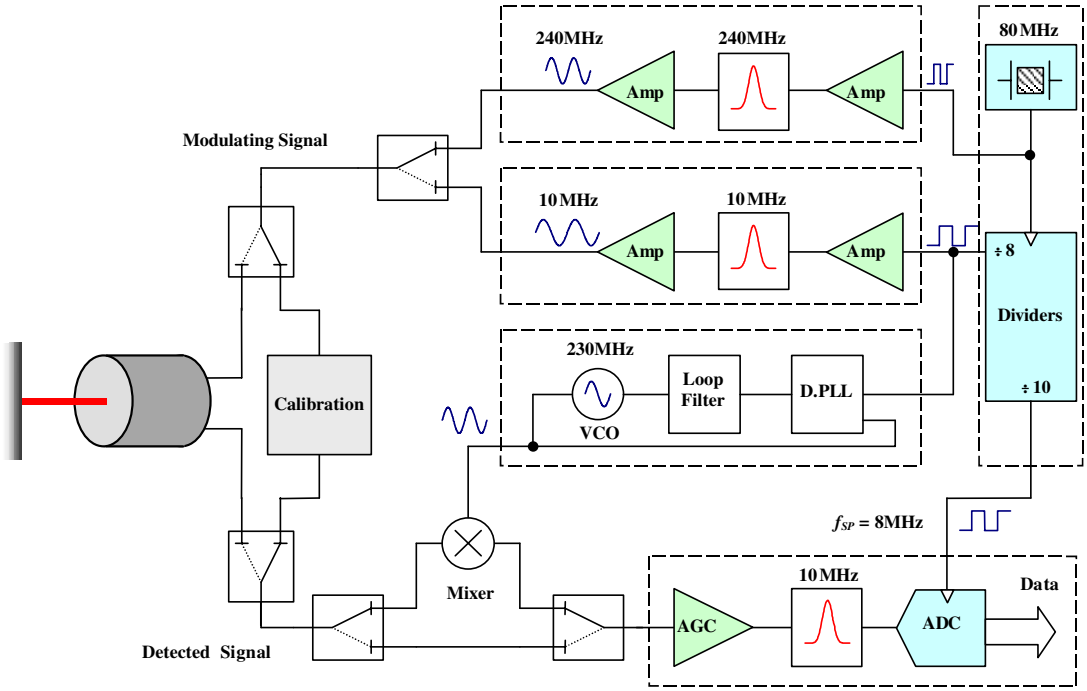

Figure 9. Structure of the whole system showing the different blocks.

measurement set with averaging of 8192 samples at 10 MHz. Otherwise it is possible to control the intensity modulation in the emitter part from the PC by tuning both bias point and amplitude modulation, but keeping a linear behaviour (a higher amplitude modulation improves the signal to noise ratio). So it seems possible to work at least with 4 mW output power and to reach 20 mW in the case of non-restrictive safety conditions.

In the case of a very low detected power the signal to noise ratio decreases. As mentioned previously the amplifier used in this prototype is the CLC5506 with a noise figure of 5 dB at high gain, leading to a noise power at the input of 8.7×10^{-21} W/$\sqrt{\text{Hz}}$, much lower than the noise equivalent power of the photodiode, which is about 10^{-14} W/$\sqrt{\text{Hz}}$. The noise limitation comes from the low power level of the return signal. The signal to noise ratio has been studied [11] showing its main dependence on the received optical power.

If the system works under conditions giving the best dynamic at the input of the ADC, then the 12 bits of resolution are fully used. If by changing the target, the detected signal is reduced by 10 dB, then the resolution decreases from 1/4096 to 1/410, that means less than nine bits. In a first approximation the theoretical phase-shift measurement accuracy due only to the digitization process will change from 0.04° to 0.4°! That shows it is very important to keep a constant amplitude at the input of the ADC in order to work with the best dynamic.

Measurements concerning different targets have been conducted with the same kind of optical head as described here and a network analyser as measurement instrument [12]. The average optical power was 2 mW, and the different targets, placed at a distance of 1 m, were micro-balls, or different materials such as paper (shiny or not), wood,. . .. The maximum amplitude for the detected signal has been obtained

for micro-balls and the lowest level for black matt paper, the difference between the corresponding detected levels being 60 dB. The influence of the tilt angle of the target is not very important, except for smooth metallic surfaces; micro-ball targets can be observed upto 80° in an attenuation range of less than 10 dB and matt white paper upto 60°.

As the gain of the CLC5506 can be tuned up to 26 dB, it seems that with three amplifiers altogether in the global gain control loop it is possible to maintain the level of the signals at the input of the ADC (IF sampling block) quite constant. Two amplifiers could be placed in the detector, the third one being placed at the input of the IF sampling unit; the gain is digitally controlled by the PC according to the measured amplitude (which is the second output of the synchronous detection).

5.2. Influence of temperature

Different elements in the system may have characteristics changing versus time, mainly because they are dependent on the temperature which increases after turning on the prototype.

The system is assumed to work at a fixed bias point, and components such as amplifiers, ADC or DAC have a linear behaviour. Small variations of gain or of the signal amplitude due to temperature drift do not affect the phase measurement and so, because of the synchronous detection, they do not affect the distance estimation.

Nevertheless the temperature drift is very important to take into account because it will dramatically affect the distance measurement accuracy. Firstly fluctuations of the reference frequency induce phase-shift measurement errors mainly because the measured signal is not at the centre frequency of the band-pass filter. The quartz oscillator that has been used is a commercial oscillator from IQD, the IQXO-22 at 80 MHz, for which the temperature stability is ± 100 ppm K^{-1} (that is also ± 1.25 ps K^{-1}). Let S_1 be the maximum corresponding variation. Secondly the temperature influences the values of inductances and capacities used for the band-pass filter. The temperature sensibility for capacities is ± 30 ppm K^{-1} and for inductances it is (220 ± 220) ppm K^{-1}. Let S_2 be the maximum corresponding variation. As there are two band-pass filters (one to realize the sine signal $S_E(t)$ from a square signal at 10 MHz and one at the input of the IF sampling unit) the worst case corresponds to a total variation of $S = 2(|S_1| + |S_2|)$.

From simulated worst-case analysis it has been estimated that between 10 and 50 °C $S_1 \approx 0.15°\ K^{-1}$ and $S_2 \approx 0.2°\ K^{-1}$ leading to $S \approx 0.7°\ K^{-1}$ and $\delta d_{\max} \approx 29$ mm K^{-1} (that means a relative error of 2×10^{-3} in the whole 15 m range).

This variation is very important but it has been determined as the worst case. Nevertheless it is necessary to reduce it. For the quartz oscillator the solution is to use a temperature compensated crystal oscillator (TCXO), available now with temperature stability as low as ± 1 ppm (see products from Vectron). Temperature effects on L and C values are much slower, because of their thermal time constant, and so a compensation by way of a calibration process should be the solution.

5.3. Calibration process

The first kind of calibration to be performed is pure electronic calibration, switching the modulation signal directly to the IF sampling unit, as shown in figure 9. There will be two calibrations for both f_{0L} and f_{0H}. These calibrations could be performed with a period of 1 s at the beginning of the prototype operation, when the temperature increases quickly, and then they could be more time spaced as the temperature is stabilized. Algorithms have been proposed for real-time calibration [13].

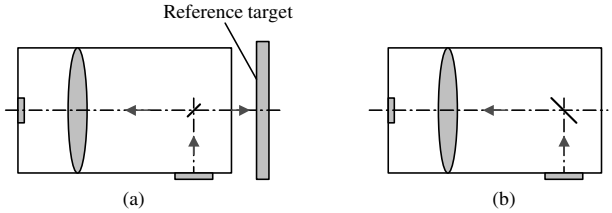

Figure 10. Optical calibration using a fixed reference target (*a*), or by changing the laser beam direction (*b*).

The second calibration is an optical calibration, with two possible techniques. The first one is to put a well known target at a known distance and to make a measurement. For example, this target could be placed just at the output of the prototype as shown in figure 10(*a*). The second possibility is to change the direction of the laser beam at the output of the small periscope (figure 10(*b*)). The corresponding modification of the optical path has also to be controlled by the computer and included in a global tuning process.

6. Conclusion

A twofold modulation frequency laser range-finder prototype has been presented in this paper. The system is based on phase-shift measurement by the use of the IF sampling technique, moving the digitization process very close to the sensing part (the optical head) and associating the under-sampling technique with digital synchronous detection. The choice of sampling frequency with respect to the modulation frequency leads to a great simplification of the digital process. The first modulation frequency is 10 MHz, leading to a global non-ambiguity range of 15 m, and the second one is 240 MHz. The choice of the frequencies and the way to synthesize them leads to a simple conception with only one PLL, reducing the global phase noise compared to an analog phase-shift measurement system based on the pure heterodyne technique. The system is designed with only one IF sampling unit operating at 10 MHz input frequency and 8 MHz sampling frequency showing an experimental standard deviation of only 0.12° for phase estimation. The resolution of the measurement is improved and for an expected final standard deviation of 0.2° in phase the standard deviation for distance is about 0.35 mm (obtained at 240 MHz). In order to reduce the effects of temperature drift on phase-shift measurement accuracy a TCXO should be used for the general reference oscillator. Nevertheless a digital calibration process is required according to the temperature dependence of electronics components such as inductances and capacities used for the band-pass filters. Otherwise the high dependence of phase-shift measurement accuracy on low detected signal should be taken into account and the global gain control loop should include enough amplifiers to maintain the signal at the input of the ADC quite constant. Knowledge of both the distance and the attenuation factor, which is information

on the surface of the target, may lead to a laser imaging system, on the condition that a scanning module is introduced. Such a system may be used for non-destructive testing or for indoor robotic control. Another important feature of this system is to be rather low cost. Finally such a prototype could be considered as a first step on the way to realize a smart laser range finder because of the different digital tuning possibilities.

References

[1] Yakolev V V 1993 High-precision laser range finders and laser systems for industrial use *Sov. J. Opt. Technol.* **60** 720–4

[2] Garcia E, Lamela H and Lopez J R 1997 A 3-D vision system for autonomous robot applications based on a low power semiconductor laser range finder *Proc. IEEE/IECON'97 (New Orleans, 1997)* vol 3 pp 1474–7

[3] Hancock J, Hoffman E, Sullivan R, Ingimarson D, Langer D and Hebert M 1997 High-performance laser range scanner *Proc. SPIE, Intelligent Transportation Systems (Pittsburgh, PA, 1997)* vol 3207 pp 40–9

[4] Journet B and Poujouly S 1998 High resolution laser range-finder based on phase-shift measurement method *Proc. SPIE Three-Dimensional Imaging and Laser-Based Systems for Metrology and Inspection IV (Boston, MA, 1998)* vol 3520 pp 123–32

[5] Pfeifer T and Gloeckner C 1999 Applications for a new laser based straightness metrology system *Proc. IMEKO-SPIE LaserMetrology'1999 (Florianopolis, 1999)* pp 1.21–1.32

[6] Kester W 1995 Undersampling applications *Practical Analog Design Techniques* (Analog Devices)

[7] Kester W 1995 High speed ADC applications in digital receivers *Practical Analog Design Techniques* (Analog Devices)

[8] Wang Feixue, Yong Shaowei and Guo Guirong 1998 Mixer-free digital quadrature demodulation based on second-order sampling *Electron. Lett.* **34** 854–5

[9] Frolich C, Mettenleiter M and Haerlt F 1997 Imaging laser radar for high-speed monitoring of the environment *Proc. SPIE, Intelligent Transportation Systems (Pittsburgh, PA, 1997)* vol 3207 pp 50–64

[10] Eugene B and Hogenauer 1991 An economical class of digital filters for decimation and interpolation *IEEE Trans. Acoust. Speech Signal Process.* **29** 155–62

[11] Koskinen M, Kostamovaara J and Myllyla R 1991 Comparison of the continuous wave and pulsed time-of-flight laser rangefinding techniques *Proc. Optics Illumination and Image Sensing for Machine Vision VI (Boston, MA, 1991)* pp 296–305

[12] Bazin G, Journet B and Placko D 1998 Non-destructive controls with a network analyser and a simple laser rangefinder *J. Opt.* **29** 206–11

[13] Sondej T and Pelka R 2001 Data processing and calibration in precision laser rangefinder *Proc. IEEE/LEOS ODIMAP III (Pavia, 2001)* pp 124–9